



A Review on SIW and Its Applications to Microwave Components

Augustine O. Nwajana ^{1,*}  and Emenike Raymond Obi ² ¹ School of Engineering, University of Greenwich, London SE10 9LS, UK² RaySoft AssetAnalytics, Regina, SK S4N 7S1, Canada; ray.obi@raysoft-aa.net

* Correspondence: a.nwajana@ieee.org; Tel.: +44-16-3488-3648

Abstract: Substrate-integrated waveguide (SIW) is a modern day (21st century) transmission line that has recently been developed. This technology has introduced new possibilities to the design of efficient circuits and components operating in the radio frequency (RF) and microwave frequency spectrum. Microstrip components are very good for low frequency applications but are ineffective at extreme frequencies, and involve rigorous fabrication concessions in the implementation of RF, microwave, and millimeter-wave components. This is due to wavelengths being short at higher frequencies. Waveguide devices, on the other hand, are ideal for higher frequency systems, but are very costly, hard to fabricate, and challenging to integrate with planar components in the neighborhood. SIW connects the gap that existed between conventional air-filled rectangular waveguide and planar transmission line technologies including the microstrip. This study explores the current advancements and new opportunities in SIW implementation of RF and microwave devices including filters, multiplexers (diplexers and triplexers), power dividers/combiners, antennas, and sensors for modern communication systems.

Keywords: radio frequency; filter; diplexer; triplexer; power divider/combiner; antennas; sensors; substrate-integrated waveguide



Citation: Nwajana, A.O.; Obi, E.R. A Review on SIW and Its Applications to Microwave Components.

Electronics **2022**, *11*, 1160. <https://doi.org/10.3390/electronics11071160>

Academic Editor: Giovanni Andrea Casula

Received: 20 March 2022

Accepted: 4 April 2022

Published: 6 April 2022

Publisher's Note: MDPI stays neutral with regard to jurisdictional claims in published maps and institutional affiliations.



Copyright: © 2022 by the authors. Licensee MDPI, Basel, Switzerland. This article is an open access article distributed under the terms and conditions of the Creative Commons Attribution (CC BY) license (<https://creativecommons.org/licenses/by/4.0/>).

1. Introduction

The electromagnetic (EM) spectrum is becoming overcrowded and is heavily crammed with a variety of wireless signals and other communication and sensing circuits and devices [1]. Electromagnetic waves of frequencies varying from 300 MHz up to 300 GHz stay classified as microwaves. This frequency span matches the free space wavelengths of 1 m to 1 mm, in that order. Electromagnetic waves of frequencies varying from 30 GHz to 300 GHz stay classified as millimetre-waves due to having wavelengths that lay directly over 1 mm and directly under 10 mm. The RF band falls somewhere beneath the microwave range, though the border in the middle of the radio frequency and microwave bands is subjective and changes based on the method established for developing the band [2].

SIW transmission line [3–10] is basically a dielectric-filled waveguide implemented by two lines of conducting posts (also known as vias) implanted within a dielectric substrate, and electrically connecting the top and the bottom conducting walls [11]. The structural evolution of the SIW technology is shown in Figure 1 [3]. The evolution shows how the conventional rectangular waveguide presented in Figure 1a was modified by occupying the airspace with a dielectric material of dielectric constant, ϵ_r , as shown in Figure 1b. The structure was further modified by using metallic posts to imitate/replace the two side walls as shown in Figure 1c, to form the SIW. This paradigm shifting technology can basically be generalised as a planar transmission line that portrays waveguide characteristics, as it builds the traditional waveguide on a section of printed circuit board, substituting its metallic side-walls with two rows of metallised vias [12]. The substrate-integrated waveguide retains the benefits of a microstrip, including compactness and ease of integration, while also retaining some of the waveguide attributes, including minimal radiation loss, elevated unloaded Q-factor, and the elevated power processing capacity [13]. The very important

advantage of the SIW transmission line technology is the opportunity to combine various devices (both active and passive) on a single substrate [14].

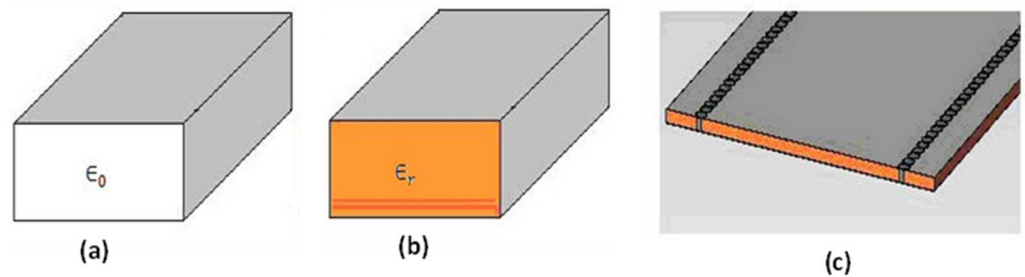


Figure 1. SIW structure development. (a) Air-filled rectangular waveguide. (b) Dielectric-filled rectangular waveguide. (c) Substrate-integrated waveguide.

2. Modes in SIW

Substrate-integrated waveguides and the traditional air-filled waveguide have comparable characteristics, as both technologies provide for $TE_{i,0}$ modes including $TE_{1,0}$, the dominant mode. Nevertheless, as opposed to the traditional air-filled waveguide which can maintain TM and $TE_{i,j}$ ($j \neq 0$) modes, the substrate-integrated waveguide is not able to maintain these modes due to the discontinuity in the side walls. Consequently, only the $TE_{i,0}$ modes can be supported in the SIW structure, as explained in [15]. The external current circulation of a conventional waveguide, with metallic posts on the thin walls, can be used to describe the fact of the presence of $TE_{1,0}$ mode in the substrate-integrated waveguide, as shown in Figure 2. This is due to surface currents being formed in guided wave constructions because of mode formation. According to [15], significant energy radiation should happen when the holes cut all the length of the current's transverse path. Alternatively, only an extremely small amount of radiation should happen when the holes cut through the path of current flow. It can be observed from Figure 2 that the holes do not cut the surface current on the side metallic wall. Hence, the $TE_{1,0}$ mode is maintained in the structure, which clarifies why the $TE_{i,0}$ modes can happen in the substrate-integrated waveguide structure.

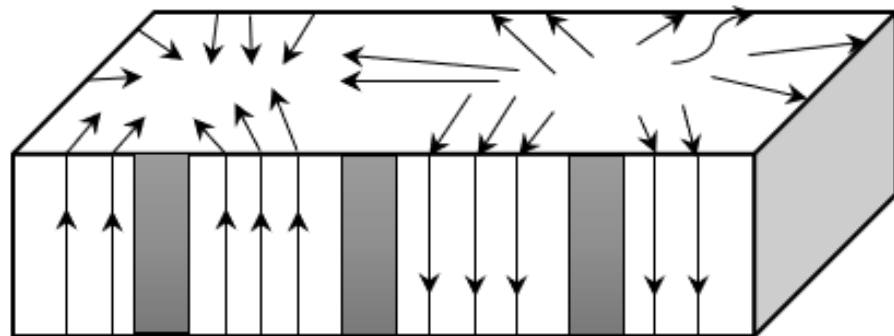


Figure 2. The $TE_{1,0}$ mode surface current distribution of a conventional rectangular waveguide with metallic holes on the thin side walls.

3. SIW Design Basics

The structure of the substrate-integrated waveguide transmission line is presented in Figure 3. This physical geometry indicates the formation of the SIW by inserting a dielectric substrate in the middle of two opposite metal plates. The side walls of the SIW structure are achieved using two lines of regular metallic vias positioned adjacent to the lengths of the substrate. This is equivalent to the metal sidewalls of the conventional waveguide.

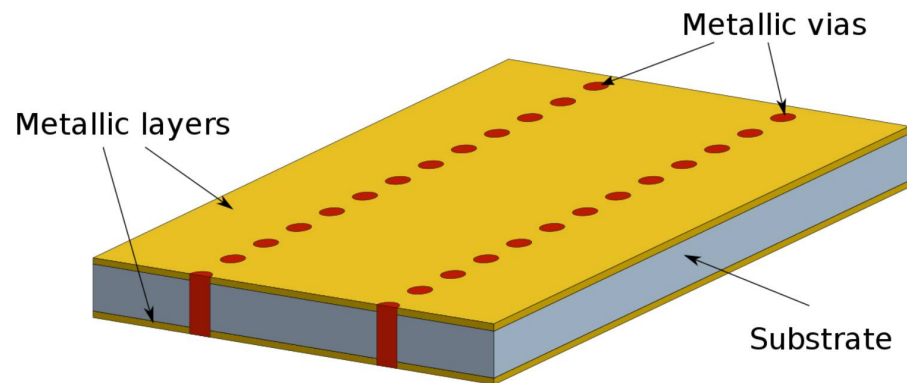


Figure 3. Physical structure of the substrate-integrated waveguide transmission line.

Three fundamental design parameters must be considered when designing the substrate-integrated waveguide to function at an assigned frequency. These parameters are shown in Figure 4 and include the substrate-integrated waveguide width, w , the metal via diameter, d , and the space or separation length between adjacent metal vias (that is, the pitch), p . Similar to the width of the conventional rectangular waveguide, the substrate-integrated waveguide width relates to the cut-off frequency of its propagation mode. The d and the p parameters define the close relationship between the substrate-integrated waveguide structure and the rectangular waveguide. Reducing the value of p to $d/2$ essentially reduces the SIW to a regular dielectric-filled waveguide. Increasing the value of p increases the amount of the SIW deviation from the conventional rectangular waveguide, with more EM energies emitting outward in the middle of the vias. Dealandes and Wu [7] show that radiation loss is negligible for an electrically small metallic via; that is, $d < 0.2\lambda$ (λ is the dielectric material wavelength), with a d/p ratio of half.

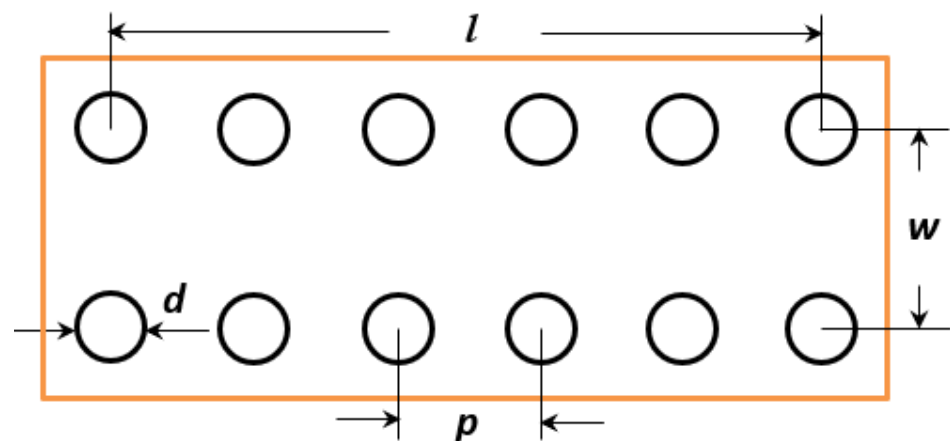


Figure 4. Substrate-integrated waveguide fundamental design parameters.

The physical size of the substrate-integrated waveguide cavity, at its basic TE_{101} mode, is calculated based on the matching resonance frequency, f_{101} as provided in Equation (1) [16]. The design parameter w_{eff} gives the substrate-integrated waveguide effective width, l_{eff} gives its effective length, μ_r is the substrate relative permeability ($\mu_r = 1$ if substrate material is non-magnetic), ϵ_r is the substrate material dielectric constant, while c_0 gives the free space speed-of-light. Experimental formulations for the w_{eff} and the l_{eff} are provided in Equation (2) [12], with the simplified versions given in Equation (3) [13,17]. It is important to note that Equations (2) and (3) are different versions of the same formula-

tion. Hence, both equations will return approximately the same value when applied in a calculation. Equation (3) is just a simplified version of Equation (2).

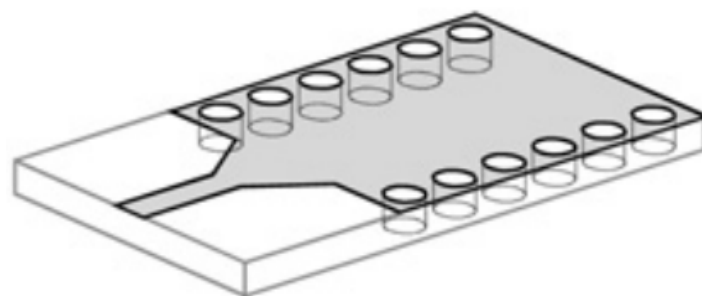
$$f_{101} = \frac{c_0}{2\pi\sqrt{\mu_r\epsilon_r}} \left[\left(\frac{\pi}{w_{eff}} \right)^2 + \left(\frac{\pi}{l_{eff}} \right)^2 \right]^{0.5} \quad (1)$$

$$\left\{ \begin{array}{l} w_{eff} = w - 1.08 \frac{d^2}{p} + 0.1 \frac{d^2}{w} \\ l_{eff} = l - 1.08 \frac{d^2}{p} + 0.1 \frac{d^2}{l} \end{array} \right\} \quad (2)$$

$$\left\{ \begin{array}{l} w_{eff} = w - \frac{d^2}{0.95p} \\ l_{eff} = l - \frac{d^2}{0.95p} \end{array} \right\} \quad (3)$$

4. Transitions in SIW

As SIW components are always integrated with other circuit components within a system, it is important to discuss the interconnection between devices. The transition sandwiched between planar transmission line technologies such as microstrips, and the substrate-integrated waveguide structure is a crucial part of the design of SIW devices [14]. A few published papers have reported SIW components with different types of input/output (i/o) connections. A microstrip to substrate-integrated waveguide transition constructed on straightforward taper was reported [18,19]. The tapered segment attaches a 50Ω microstrip signal line to the substrate-integrated waveguide. The taper is utilised by converting the quasi-TEM mode in the microstrip technology to the TE₁₀ mode of the substrate-integrated waveguide. Coplanar waveguides (CPWs) have also played a vital role in this research area. Coplanar waveguide to substrate-integrated waveguide conversion established with a ninety-degree bend was reported in [20]. In another research paper, a kind of conversion involving a grounded CPW and substrate-integrated waveguide established on a current probe was proposed [21]. Current flow across the probe produces a magnetic field which corresponds to the magnetic field within the substrate-integrated waveguide. Transition between the traditional rectangular waveguide and the substrate-integrated waveguide structure has also been proposed in [22,23]. Microstrip to substrate-integrated waveguide conversions within multiple layered substrates were researched/reported [24]. Nwajana, Yeo, and Dainkeh proposed a new microstrip–CPW–SIW transition in [10]. The new transition technique exploits the step impedance on a 50Ω microstrip signal path, to the small impedance grounded coplanar waveguide, then linking to the SIW component through the brief small impedance grounded coplanar waveguide signal path. The conversion method is effective since it facilitates double flexibilities in managing i/o couplings; hence, the external quality factor may be altered by both altering the stepped-impedance of the coplanar waveguide and the size of the brief coplanar waveguide signal path. Figure 5 shows some of the popular transition techniques that have been employed in the design of substrate-integrated waveguide components.



(a)

Figure 5. Cont.

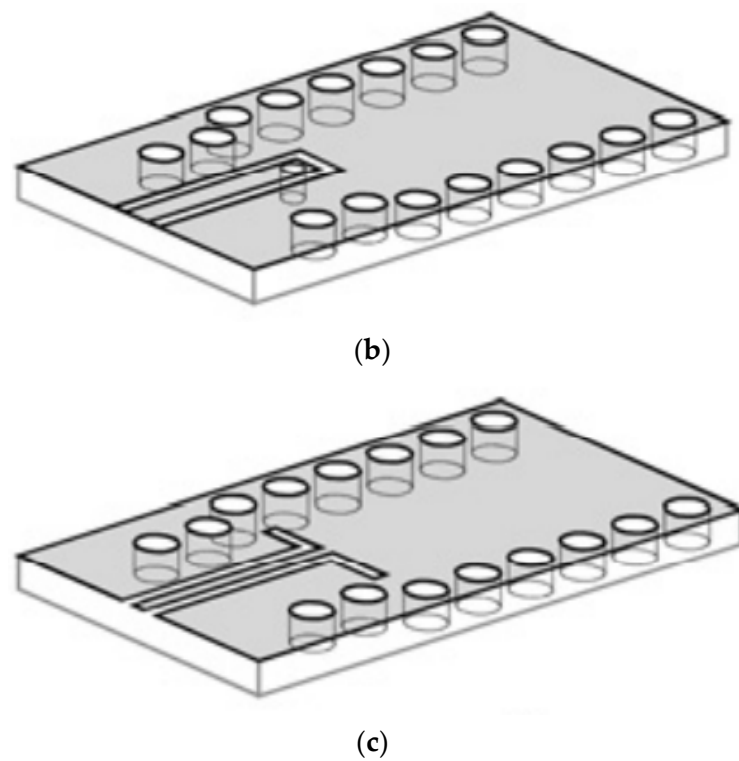


Figure 5. Some popular transitions between planar transmission lines and substrate-integrated waveguides: (a) microstrip-to-SIW transition based on a simple taper; (b) CPW-to-SIW transition based on a current probe; (c) CPW-to-SIW transition based on a ninety-degree bend [14].

5. Losses in Substrate-Integrated Waveguides

The key losses linked to SIW components are associated with three loss mechanisms including conductor loss, dielectric loss, and radiation loss [25–28]. The conductor loss is linked to the metallic walls limited conductivity; the dielectric loss is linked to the substrate material loss tangent; while the radiation loss is linked to the outflow of EM energy over the regular openings in the dual paths of metallic vias [15,29]. The conductor loss and the dielectric loss that take place in substrate-integrated waveguide components are like those that occur in rectangular waveguide components. The radiation loss, conversely, is particularly related to the substrate-integrated waveguide and is because of the regular openings in the dual paths of metal vias inserted in the dielectric substrate. One main issue in the design of a substrate-integrated waveguide component is the capability to efficiently diminish the losses, especially if the component is designed to function over the millimetre-wave band [29].

The substrate-integrated waveguide conductor loss is comparable to the conductor loss in the traditional waveguide component, and this is because of the limited conductivity of the metal edges. In [25], it was shown that a substantial decline in losses linked to conductors may be accomplished through improving the substrate depth while maintaining the remaining sizes in the substrate-integrated waveguide structure. A decrease in pitch p may also lead to a decline in conductor loss owing to the improved metallic coat [25]. SIW conductor loss may be marginally reduced by increasing the size of the metal via diameter. Attenuation constant α_c , owing to the substrate-integrated waveguide conductor loss at a specific frequency, f , may be investigated based on Equation (4) [30]; h is the dielectric substrate depth, σ_c is the metallic wall conductivity, f_0 is the SIW cavity cut-off frequency, ϵ_0 stands for the free space dielectric constant, ϵ_r stands for the substrate material dielectric constant, and w_{eff} stands for the SIW cavity effective width. As Equation (4) was initially designed for evaluating the conductor loss attenuation constant in the traditional waveguide, the effective width given in Equations (2) or (3) is used as an alternative to

the original width of the substrate-integrated waveguide [30]. This is to ensure that the equation is accurately adapted in the design of SIW components.

$$\alpha_c(f) = \frac{\sqrt{\pi f \epsilon_0 \epsilon_r}}{h \sqrt{\sigma_c}} \frac{1 + 2(f_0/f)^2 h/w_{eff}}{\sqrt{1 - (f_0/f)^2}} \quad (4)$$

The dielectric loss in substrate-integrated waveguide devices is also similar to the dielectric loss in conventional waveguide devices. The loss is entirely reliant on the dielectric substrate material loss tangent and not the physical structure of the substrate-integrated waveguide [14]; provided the depth of the substrate, h , is reduced in size when compared to a half-wavelength; h will have no impact on the dielectric loss [31]. The dielectric loss is usually the greatest provider of deficiencies in millimetre-wave components; therefore, a cautious choice when selecting the appropriate substrate material is of paramount significance. Mathematical formulation developed for the computing the dielectric loss attenuation constant in the traditional waveguide may be utilised in evaluating the dielectric loss attenuation constant α_d in the substrate-integrated waveguide. The mathematical formulation, as reported in [30], is given by Equation (5), where c_0 is the free space speed of light and $\tan \delta$ is the loss tangent of the dielectric substrate material.

$$\alpha_d = \frac{\pi f \sqrt{\epsilon_r}}{c_0 \sqrt{1 - (f_0/f)^2}} \tan \delta \quad (5)$$

SIW radiation loss, as opposed to conductor loss and dielectric loss, is overtly connected to the substrate-integrated waveguide itself. This is because of the periodic gaps occurring in the middle of the metal vias, which are implanted in the dielectric substrate [30]. The radiation loss in substrate-integrated waveguide components is due to energy outflow out of these gaps. As reported in [4], the radiation loss in substrate-integrated waveguides may be overlooked when the metalised hole diameter d and the pitch p are selected in accordance with Equation (6), where λ_g is the guided wavelength in the substrate-integrated waveguide. The condition should guarantee that radiation loss is maintained at the lowest possible level that renders it insignificant. This implies that the substrate-integrated waveguide can be developed as a traditional dielectric-filled rectangular waveguide [4].

$$d < \lambda_g/5 \quad \text{and} \quad p \leq 2d \quad (6)$$

Although Equation (6) is the proposed bare minimum requirement for substrate integrated-waveguide design, the $d \geq \lambda_g/5$ parameter value and/or the $p > 2d$ parameter value may still be employed with no devastating outcomes [4]. To achieve low radiation loss performance, [14] suggests that the ratio p/d ought to be maintained under 2.5, with an optimal substrate-integrated waveguide design having a parameter value of $p = 2d$. The radiation loss attenuation constant α_r in substrate-integrated waveguide may be investigated based on Equation (7) [32], where w stands for the substrate-integrated waveguide cavity width and λ stands for the SIW propagation wavelength. Equation (7) is centred on the mathematical simplification of the basic (quasi TE_{10}) mode of the substrate-integrated waveguide into double plane waves. This is centred on the mathematical computation of the transmission coefficient of an unlimited grid of metallic vias [30,32].

$$\alpha_r = \frac{\frac{1}{w} \left(\frac{d}{w}\right)^{2.84} \left(\frac{s}{d} - 1\right)^{6.28}}{4.85 \sqrt{\left(\frac{2w}{\lambda}\right)^2 - 1}} \quad (7)$$

6. Performance Attributes of the SIW

The substrate-integrated waveguide transmission line technology has been recently gaining huge global acceptance in microwave engineering due to its notable performance

attributes. Some of these performance characteristics of the SIW, according to Deslandes and Wu [13] include compact size, low radiation loss, ease of integration, elevated unloaded Q-factor, elevated power handling capability, thermal stability, etc. Some of these performance attributes are discussed in this section.

The physical features of microwave and millimetre-wave devices would always respond to variations in the temperature of their operating environments. This is because the materials used in the implementation and fabrication of such devices/components are naturally temperature-dependent. SIW devices have good thermal stability when compared to similar devices implemented/fabricated with other commercially available transmission lines (that is, planar transmission lines and waveguides). To achieve this thermal stability in SIW components, attention must be paid in choosing the design substrate as explained in [33]. The paper highlighted the following vital three steps for a successful thermal stability analysis in SIW component design:

- A stress assessment should be performed to obtain the physical change in dimensions in connection with environment temperature as the input;
- A full-wave field assessment should be conducted to verify the frequency shift versus the changes in the physical dimension and selected substrate permittivity;
- A redesign of the given device/component by compensating for the adjustments in the electrical parameters.

According to [34–36], assigning opposite signs to the thermal expansion coefficient of permittivity and the physical dimensional thermal expansion coefficient can lower the temperature coefficient of a given device resonant frequency provided they can both combine effectively. For any given SIW component with substrate permittivity (i.e., dielectric constant), ϵ_r , the thermal expansion coefficient in the width, α , and temperature, T , the temperature coefficients, τ_f , of the TE_{101} mode resonant frequency, f_{101} , can be determined by means of Equation (8), provided the thermal expansion coefficient in the width is equivalent to that of the length [33].

$$\tau_f(TE_{101}) = \frac{1}{f} \frac{\delta f}{\delta T} = - \left(\frac{1}{2} \frac{1}{\epsilon_r} \frac{\delta \epsilon_r}{\delta T} + \frac{1}{\alpha} \frac{\delta \alpha}{\delta T} \right) \quad (8)$$

The power handling performance of SIW devices/components makes the technology a preferred choice in the modelling, execution, and fabrication of microwave and millimetre-wave components operating in environments with high humidity [36]. According to [37,38], microwave and millimetre-wave devices/components may dispel a considerable quantity of power, resulting to a general rise in temperature and local hot spots. This issue is a major contributing factor in the aging of a device structure in relation to the substrate material. For SIW filtering components including filters, multiplexers (e.g., diplexer/triplexers), filtering power dividers/combiners, filtering antennas, etc., the mean power handling capability is dependent on the filtering order, geometry, topology, bandwidth, and resonator unloaded quality factor. The authors of [38] gave the seven steps to apply when evaluating the average power handling ability of a substrate-integrated waveguide filtering device as follows:

- A full-wave field assessment should be conducted to establish the power dissipation and its allocation;
- The dispersed power should be employed in the performance of a thermal assessment and the temperature increase and local hot spots established;
- A comparison of the worst-case values to the glass transition temperature of the substrate at which the material adjusts its performance from being glassy to being rubbery;
- The determination and application of the safety limits;
- A stress assessment should be performed to achieve the physical dimensional adjustment for the temperature allocation under extreme mean power;
- A full-wave field assessment should be conducted to establish the frequency shift along with the shift in bandwidth and return loss, using the revised dimension and substrate permittivity,

- A redesign of the given device/component by compensating for the adjustments in the electrical parameters.

7. Substrate Selection for SIW Implementation

In the design of substrate-integrated waveguide devices/components, substrate selection is considered vital for the structural and electrical performance in comparison to other types of transmission line structures including microstrips, coplanar waveguides, etc. Using an SIW filter as a case study, Chen and Wu [33] showed the relationship between the device substrate features and the size, the insertion loss, the thermal stability, the mean power management capability, and the peak power management capability.

- The physical size of an SIW device is directly linked to the permittivity or dielectric constant of the material used for the device implementation. The higher the material dielectric constant, the smaller the physical size of the SIW device.
- The amount of insertion loss observed in an SIW device relates to three factors: substrate thickness, dielectric loss, and copper foil.
- Thermal expansion and thermal coefficient of permittivity of a substrate material determines the temperature stability of an SIW device.
- SIW components are well known for their good power handling capabilities. The average power handling capability is based on the substrate thermal expansion, the thermal coefficient of permittivity, the thermal conductivity, and the glass transition temperature, while the peak power handling capability is only linked to the substrate dielectric strength.

It is important to understand that the utilisation of a particular type of substrate in the SIW components design will also depend on the method employed in the component development. Hence, several parts of the SIW component design and implementation are interrelated.

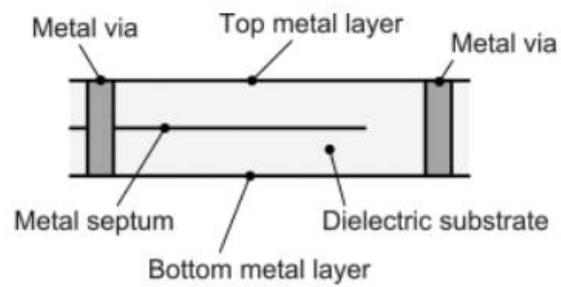
8. Evolutionary Structures of the SIW

The conventional structure of the SIW has some limitations that can be linked to its evolution from the rectangular waveguide. Some of these limitations are associated with the bandwidth and compactness of the physical structure of the SIW, as explained in [39]. Several researchers have worked tirelessly to help mitigate said limitations by proposing and investigating alternative and more compact SIW structures, as reported in [14,39,40].

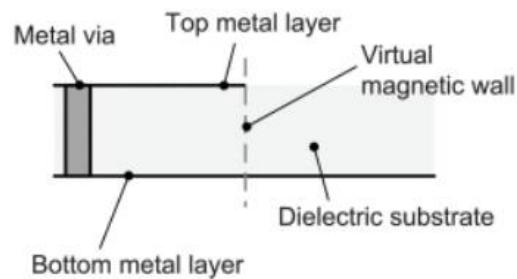
One of the modified SIW structures reported in [41–48] is the substrate-integrated folded waveguide (SIFW) as indicated in Figure 6a. This version of the SIW allows for a 50% decrease in the physical size of a device due to the folded structure. The downside of this version of the SIW is that it exhibits a slightly higher loss mechanisms when compared to the standard/conventional version. The folding of the structure also means the requirement for a dual-layer fabrication process which is slightly more complex when compared to a single-layer fabrication process.

Another modified version of the SIW is reported in [49–55]. This version is known to as the half-mode SIW (HMSIW) as shown in Figure 6b. This version also allows for a 50% decrease in the physical dimension of a device such as the SIFW. However, unlike the SIFW, this version uses a symmetry plane to replace half of the standard SIW structure. The symmetry plane acts as a virtual magnetic wall used to replace one half of the physical structure. This means that the HMSIW, like the standard SIW, is also manufactured using the single-layer manufacturing process. This is an added advantage over the SIFW.

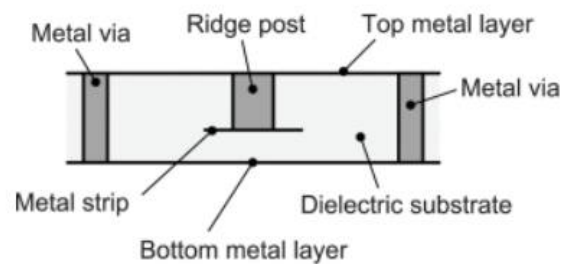
The substrate-integrated ridge waveguide (SIRW) is another evolution of the standard SIW that has been investigated and reported in [56–60]. This version has the physical structure given in Figure 6c. The SIRW is a version of the SIW where a ridge is realised using a row of thin, partial-height metallic vias positioned in the centre of the extended side of the SIW. This topology of the SIRW ensures that bandwidth improvement and compactness are achieved in an SIW device.



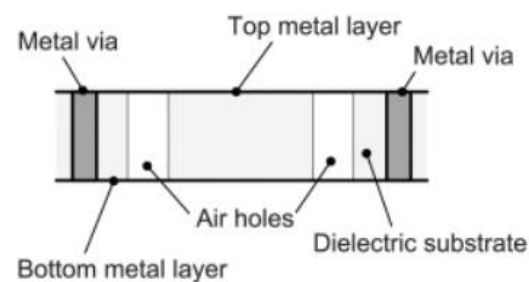
(a)



(b)



(c)



(d)

Figure 6. Cross section of the different versions of the compact SIW structures: (a) substrate-integrated folded waveguide; (b) half-mode substrate-integrated waveguide; (c) substrate-integrated ridge waveguide; (d) substrate-integrated slab waveguide [14].

One other modified version of the SIW that has been investigated and reported in [61–65] is the substrate-integrated slab waveguide (SISW) as given in Figure 6d. In this evolution of the SIW, the dielectric material is regularly perforated with air-filled vias which are in the horizontal section of the SIW. A further significant reduction in the physical size of a SIW device has been reported in [66], where the folded half-mode substrate-integrated

waveguide (FHMSIW) was used to implement a 3 dB coupler, hence further reducing the physical device size to almost half of the equivalent HMSIW coupler device.

9. SIW Filter

The modern-day EM spectrum is becoming overcrowded and heavily inhabited with numerous wireless signals and parasitic interferers in connection with transmission and sensing services. Progressively more advanced RF, microwave, and millimetre-wave filters are essential to facilitate the passing and/or stopping of particular signals [1]. A bandpass filter selects frequency signals in a particular channel while discarding all other frequency signals external to the channel. The main function of a bandpass filter in the transmitter is to reduce the bandwidth of the output signal to the channel allocated for the transmission. Due to this, the transmitter is blocked from intruding on other stations. In the receiver, a channel filter allows signals within a specified range of frequencies to be received and interpreted, while preventing signals at unwanted frequencies from going through.

SIW filters have recently been receiving particular attention and numerous design techniques and topologies have been reported in the literature. All reported SIW filter design methods involve some sort of compromise in choosing which crucial design specifications to prioritise, including size, selectivity, power handling capability, quality factor, cost, sensitivity to environmental effects, and other performance metrics (e.g., in-band and out-band performance metrics). It is practically challenging, if not impractical, to concurrently achieve all these conflicting design requirements. Attaining higher band selectivity, for example, normally involves the use of additional resonators which implies greater insertion loss along the communication channel [67]. A collection of SIW filter design techniques were recently suggested as modifications of the conventional substrate integration waveguide filter shown in Figure 7 and reported in [67]. These variations including the dual-mode SIW filters [68,69], the wideband SIW filters [68], the multi-band SIW filters [70,71], and the reconfigurable SIW filters [72].

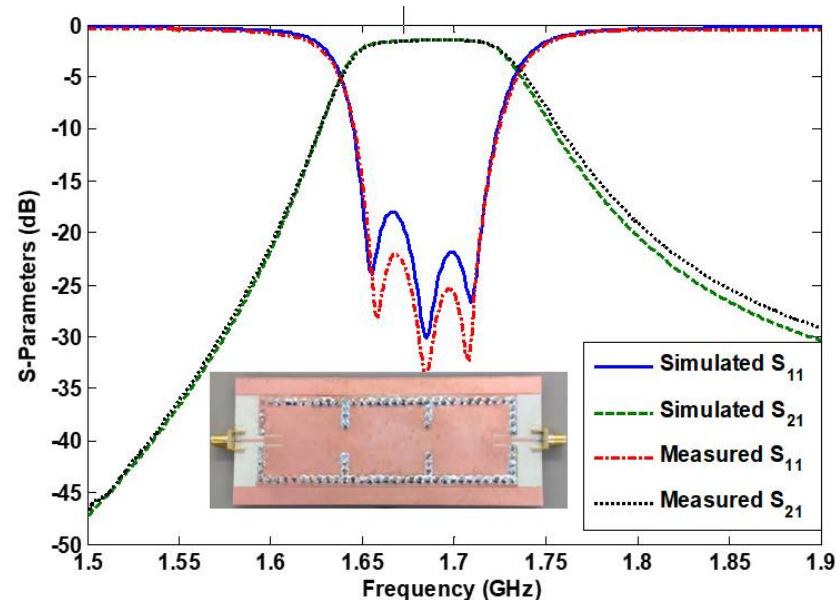
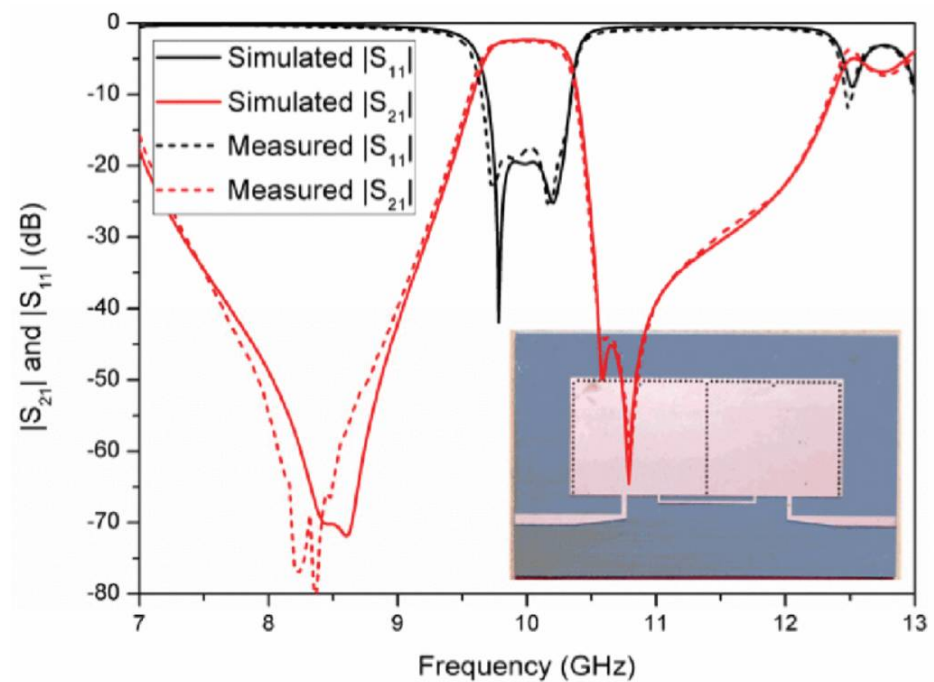


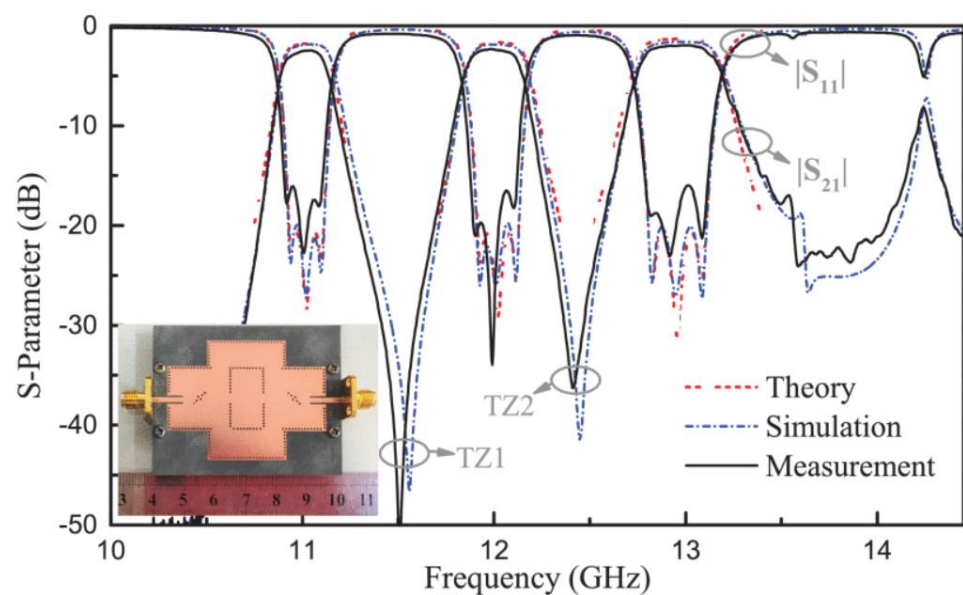
Figure 7. Simulation and measurement responses of a conventional three-pole SIW filter including the image of the fabricated filter device.

Dual-mode SIW filters are primarily developed to decrease the filter volume by at least 50% [68] when compared to the conventional SIW filter [67]. This means that a reduced filter transmission loss is guaranteed due to the halved number of resonating SIW cavities. Dual-mode SIW filters could further achieve compactness when implemented on half-mode SIW cavities as reported in [49] and shown in Figure 8a. A dual-mode SIW filter with flexible responses has also been suggested in [69]. The proposed technique achieved many

adjustable transmission zeros. It also maintains the integrity and shielding of the SIW without increasing the design complexity [69].



(a)



(b)

Figure 8. Simulation and measurement responses and the image of the fabricated SIW filters: (a) four-pole half-mode SIW bandpass filter. Reprinted/adapted with permission from Ref. [49]. 2021, F. Zhu et al.; (b) third-order triple-band bandpass filter [72].

Wideband substrate-integrated waveguide filters have been proposed and achieved with the transverse electromagnetic (TEM) mode transmission line because of their dispersion-free, broadband, and single-mode performance. A substrate-integrated waveguide allows only the propagation of TE modes which make the design of wideband SIW filters simpler and more achievable without the design consideration of parasitic TM modes. To increase

the coupling for wideband applications, a zigzag filter topology with 28% bandwidth for European ultrawideband (UWB) applications was reported in [70]. Additional controllable cross-coupling networks are realised by both physical and nonphysical approaches to realise sharper results and more flexible alteration of the transmission zeros. A quick and correct full-wave EM analysis technique based on the boundary integral-resonant mode expansion technique was proposed and established to design the filter [68].

Multi-band SIW filters including the dual-band bandpass filter [71] and triple-band bandpass filter shown in Figure 8b [72] have been reported. These design topologies are progressively becoming essential with the contemporary fast growth, development, and advancement in multi-band wireless communication systems. This type of filter is helpful in separating a small portion of a frequency band in a larger band. Reconfigurable SIW filters [73] are important for future multi-functional radio and radar systems, including smart and cognitive radio and radar systems that abound across commercial, civilian, and defence sectors. They are popular in the control and better use of the radiofrequency spectrum [68]. A performance comparison of published works on SIW filters is given in Table 1.

Table 1. Performance comparison of published works on SIW filters.

Ref.	f_0 (GHz)	Filter Order	No. of Bands	Insertion Loss (dB)	Return Loss (dB)	Dimension ($\lambda_0 \times \lambda_0$)
[67]	1.7	3	1	1.3	22	0.27×0.63
[69]	25/27	4	2	1.7/1.6	14	-
[70]	7.5	5	1	1.5	19	-
[71]	8/11.4	3	2	2.3/3.1	16	1.66×1.31
[72]	11/12/13	5	3	3.7/3.8/2.5	14.4	3.88×2.17

10. SIW Multiplexer

Multiplexers are microwave components employed for both breaking a frequency spectrum into two or more sub-spectrums or for merging two or more sub-spectrums into one wide spectrum. Diplexers are commonly employed in satellite communication applications to merge the transmit and the receive antennas on space vehicles [17]. This marginally lowers the size of the space vehicle by a sizeable quantity. Triplexers, on the other hand, are for linking three separate networks with distinct operational frequencies to one port [72]. Multiplexers are normally used in the RF front end of cellular radio base stations to divide the transmit and the receive channels.

Conventional SIW multiplexers (including diplexers and triplexers) are composed of several coupled single-mode SIW cavities/resonators with separate paths and a matching network as reported in [17]. Multi-mode resonators, such as the dual-mode resonator proposed in [74] and the triple-mode cavity reported in [75], have been investigated and implemented to enormously miniaturise the end device, and reduce the extent of losses recorded on the transmit/receive paths. SIW diplexers based on circular triplet combline filters have been proposed in [76]. The involvement of the cross-couplings in the circular triplet section was used to realise high rejection in the diplexer device. A tuneable multi-layer SIW diplexer has been reported in [77] with simulation and measurement responses shown in Figure 9. The multi-layer architecture in the design facilitated the easy control of the electric and magnetic coupling via circular slots. This allowed for a wide stopband to be achieved in the SIW diplexer component. A performance comparison of published works on SIW diplexers is given in Table 2.

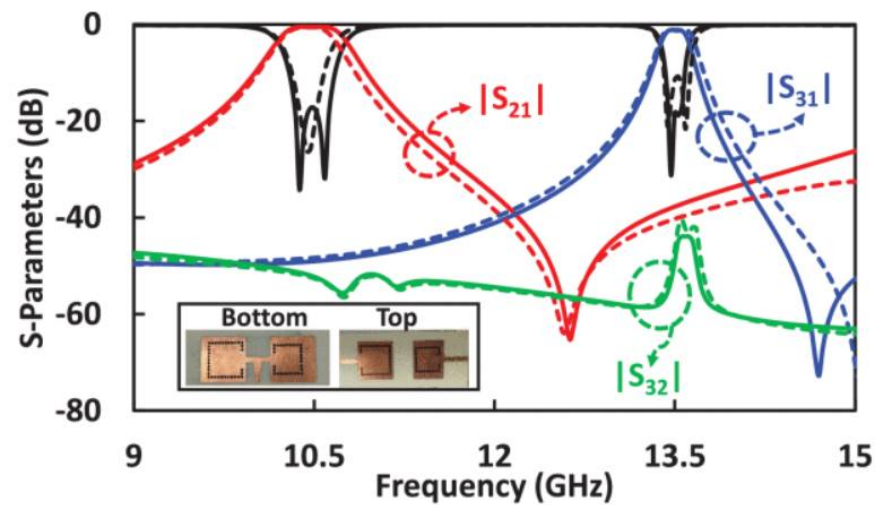


Figure 9. Simulation and measurement responses of a tuneable SIW diplexer including the images of the fabricated filter component. Reprinted/adapted with permission from Ref. [77]. 2019, A. Iqbal et al.

Table 2. Performance comparison of published works on SIW diplexers.

Ref.	f_1/f_2 (GHz)	Filtering Order	Isolation (dB)	Insertion Loss (dB)	Return Loss (dB)	Dimension ($\lambda_o \times \lambda_o$)
[17]	1.7/1.9	5	>50	2.86/2.91	15/12	-
[74]	5/5.25	2	>45	2.2/2.4	17/15	1.02×2.08
[74]	5/5.25	2	>40	1.8/1.5	16/18	1.02×2.08
[76]	9.5/10.5	3	>35	1.6/2.1	17/16	2.04×0.65
[77]	10.5/13.5	3	>42	0.9/1.4	14.4	2.14×1.30

11. SIW Power Divider/Combiner

Power dividers are microwave passive components that receive input signals and provide several output signals with phase and amplitude characteristics [78,79]. These components can be operated as power combiners by simply supplying signals into the divider output ports. The vector summation of the signals will appear as a single output at the divider's input port. Integrating power dividers/combiners (PDCs) and channel filters into a single component does not only reduce the physical footprint of the component, but also helps to significantly reduce losses. The reason is that integrated filtering PDCs [80–82] reduce the number of lossy connectors within a communication system, since the filter and the PDC exist as a single integrated device. It has been reported in the literature [78] that Y-junction-based power dividers provide a wider bandwidth of 25.2% when compared to T-junction [83]-based power dividers which provide 10.2% bandwidth.

Various classes of SIW-based power divider/combiners have been reported in [78], including corporate (Tree), Series, multimode interference, half-mode SIW, Magic-T, radial cavity, Wilkinson and Gysel SIW power dividers. Filtering power dividers with tuneable and reconfigurable passbands has been proposed in [81], where tuneable resonators are employed to ensure the device can be used for reconfigurable applications. SIW-adjustable filtering power dividers have also been proposed in [82]. The design is based on multi-layer SIW and achieved both equal and unequal power division as shown in Figure 10. The design combines three similar slotline–microstrip transition structures containing two rectangular resonators, achieving the filtering power division responses as explained in [82]. A performance comparison of published works on SIW power dividers/combiners is given in Table 3.

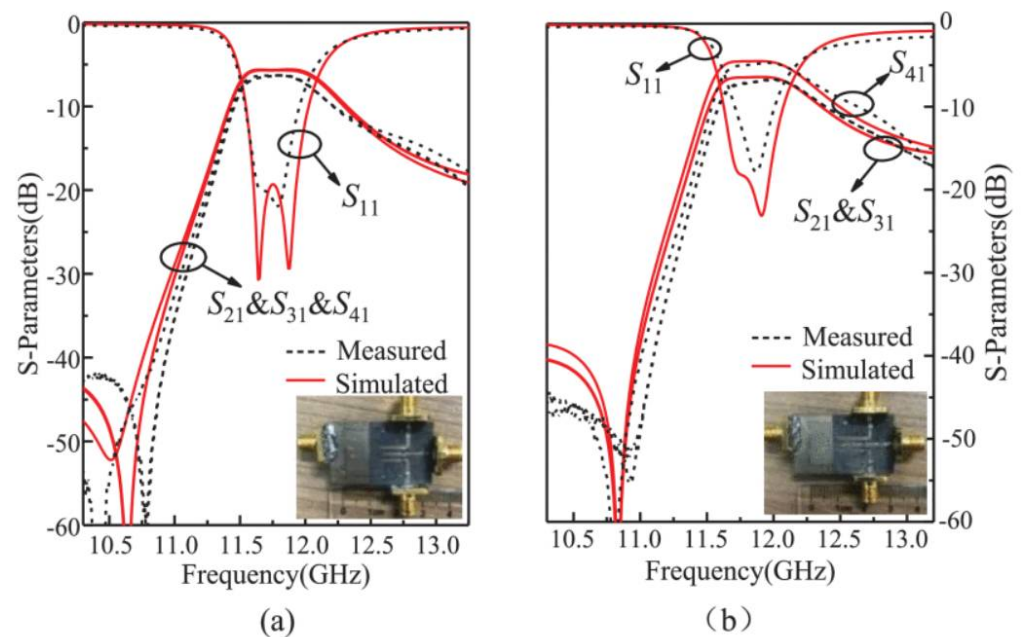


Figure 10. Simulation and measurement responses and images of the fabricated SIW filtering power divider: (a) with equal power division; (b) with unequal power division. Reprinted/adapted with permission from Ref. [82]. 2020, G. Zhang et al.

Table 3. Performance comparison of published works on SIW power dividers/combiners.

Ref.	f_0 (GHz)	Filtering Property	No. of Bands	Insolation (dB)	Return Loss (dB)	Dimension ($\lambda_o \times \lambda_o$)
[79]	3.5/4.7/6.3	No	3	>14	>20	0.03×1.0
[79]	3.3/4.8/6.2/7.7	No	4	>12	>19	0.02×1.0
[80]	5.9/6.4	Yes	2	>21	>20	0.77×1.0
[81]	1.7/2.85	Yes	2	>13	>15	0.28×0.28
[82]	11.8	Yes	3	>16.8	>18	1.47×0.87

12. SIW Antennas

Antennas are the key components in wireless communication systems. Their main function is to transmit and receive signals. Further to the increasing trend concerning simplicity and miniaturisation of communication systems, it is necessary to merge antennas and filters into a solitary device that simultaneously achieves both radiating and filtering functionalities, as shown in Figure 11. This integrated device is known as a filtering antenna (or filtenna). The filtenna lessens the pre-filtering condition and advances the noise performance of the system.

Substrate-integrated waveguide filtering antennas are currently receiving a wide range of interest and have been achieved using different design techniques. Studies [84–86] proposed single band SIW filtennas with controllable radiation nulls. The radiation nulls enhance the radiation features of the filtering antennas. Electric and magnetic combined coupling structures and basic modes were used to generate two radiation nulls as explained in [84]. The two radiation nulls may be independently operated to attain elevated selectivity and flexibility in the suggested filtenna, as explained in [85]. Dual-band SIW filtering antennas have also been reported [87–89]. These type of filtennas have the added advantage of improved out-of-band suppression, with a multifunctional single slot. The etched multifunctional slot helps to improve the out-of-band suppression and the radiation gain. SIW filtennas have also been proposed and designed for millimetre-wave applications [90–93]. A performance-improved filtenna was exploited in [90] to act as the source of a 60 GHz

Fabry–Perot Cavity antenna. This greatly improved the filtering function of the proposed filter. Compact size and low insertion loss was achieved in [91] by using eight-mode SIW cavities fully shielded by metallised vias. Multilayer SIW structures have also been employed in the design of antennas as reported in [92]. The structure consists of an SIW feed with a coupling slot, differential-fed L-shaped probes, and radiating patches. The authors of [93] proposed an antipodal linearly tapered slot filter antenna with diverse split-ring resonators. The proposed design achieved a lower band suppression between 23.5 and 27.5 GHz. An SIW antenna based on negative order resonance is reported in [94]. The major difference between the antenna reported in [94] and those reported in [84–93] is the absence of the integrated filtering property in [94]. This simply means that, while the antennas in [84–93] will radiate energy as well as filter out unwanted frequencies, the antenna reported in [94] will only radiate energy, while depending on separately designed filters for frequency filtering. A performance comparison of published works on SIW antennas is given in Table 4.

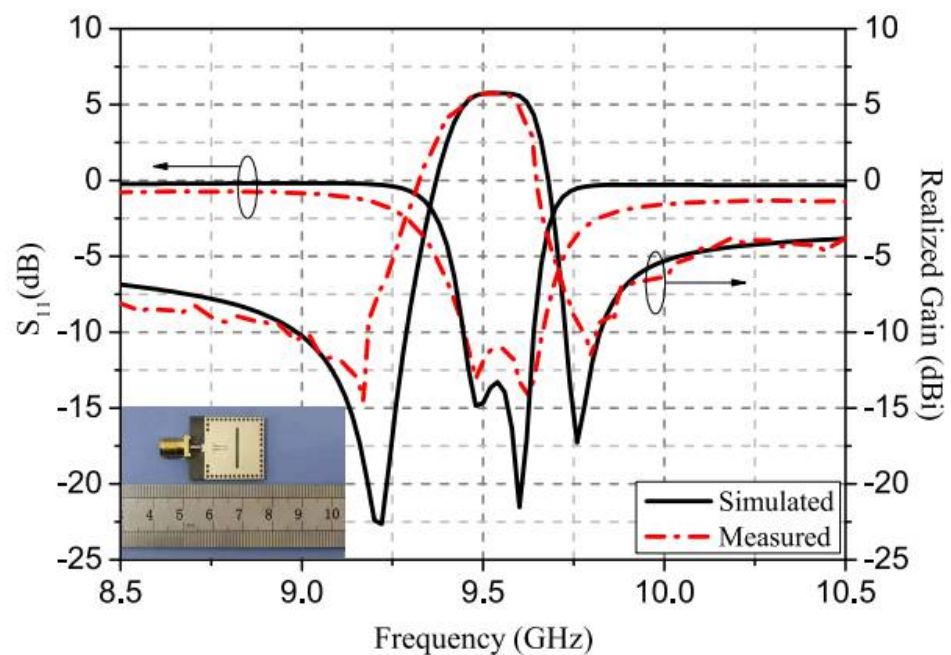


Figure 11. Image, simulation, and measurement responses of a filtering antenna [84].

Table 4. Performance comparison of published works on SIW antennas.

Ref.	f_0 (GHz)	Filtering Property	No. of Poles	No. of Bands	Fractional Bandwidth (%)	Gain (dBi)	Polarisation in Both E- and H-Planes (dB)	Dimension ($\lambda_o \times \lambda_o$)
[84]	9.6	Yes	2	1	2.53	5.8	>20	-
[85]	5.365	Yes	4	1	7.64	5.3	>20	0.9×1.1
[86]	11.8	Yes	3	1	11.84	5.0	-	0.48×0.47
[87]	3.59/4.11	Yes	4	2	2.3	4.84	>16	1.3×1.1
[92]	27.5	Yes	3	1	25.8	8.9	>29	3.94×3.26
[93]	25.5	Yes	2	1	15.6	10.05	-	2.17×0.8
[94]	7.25	No	-	-	1.52	3.16	>12.5	0.265×0.318

13. SIW Sensors

Sensors and wireless identification are modern technologies with a wide range of applications. Some popular utilisations include indoor and outdoor tracking, sensing, operation of tags attached objects, human bodies, etc. Sensing and wireless identification

of people and physical objects has enabled them to become smartly connected. This has led to scientific breakthroughs in various fields of human endeavours including healthcare, health monitoring, disaster monitoring, logistics, social networking, smart environments, security services, etc.

Substrate-integrated waveguides have been widely employed in achieving humidity sensors [95] and rotation sensors [96] due to their improved performance and accuracy. Microstrip-based sensors [97] normally exhibit poor quality factors and moderate sensitivity. This explains why their use is limited to testing of only medium to high-loss dielectric materials as explained in [98–101]. The SIW sensor reported in [98] was excited using an external coupling topology incorporating a transition offset. The sensor exhibits yielding at high sensitivity of 20 MHz which is equivalent to 0.67% in terms of normalised sensitivity [98]. An SIW-based sensor with negative order resonance is reported in [102]. The sensor is reported to be “compact dielectric-permittivity of liquid samples”. The sensor was implemented using SIW and achieved a compact footprint of $(0.25 \times 0.42)\lambda_0$, where λ_0 is the wavelength in free-space at the sensor’s operating frequency. The image and experimental resonant curves of one of the designed sensors (that is, sensor A) for various samples is shown in Figure 12. A performance comparison of published works on SIW sensors is given in Table 5.

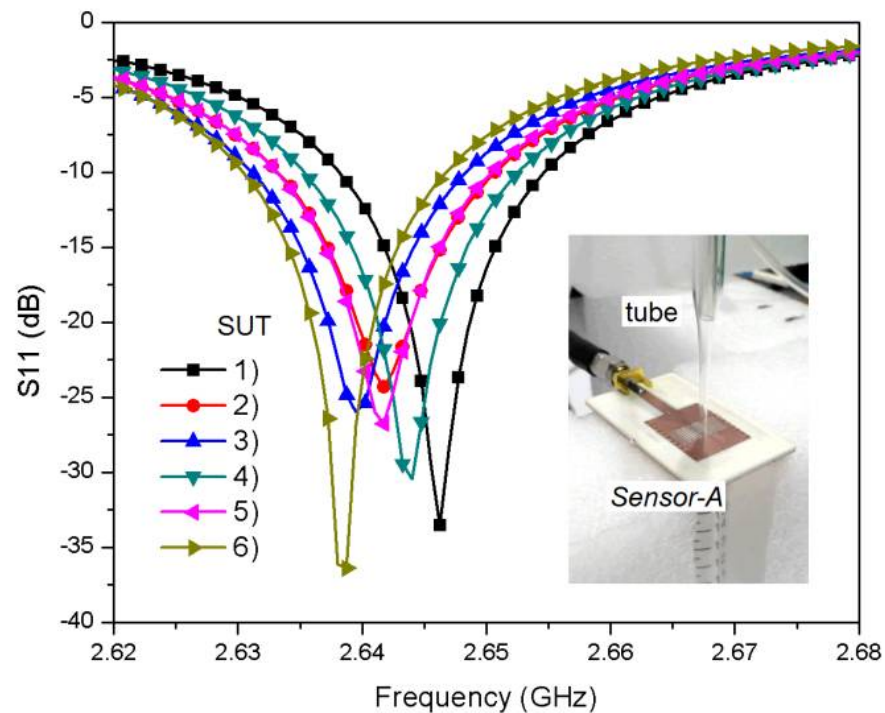


Figure 12. Image and experimental resonant curves for sensor A using various samples. Reprinted/adapted with permission from Ref. [102]. 2019, H.L. Morales.

Table 5. Performance comparison of published works on SIW sensors.

Ref.	Operating Frequency (GHz)	Dimension ($\lambda_0 \times \lambda_0$)	Application	Quality Factor Achieved
[97]	~ 5.0	0.191×0.205	Crack detection in metallic materials	>148
[98]	~ 3.0	-	Permittivity estimation of dielectric substrate materials	>515
[99]	~ 7.0	-	Complex permittivity measurement	>517
[100]	~ 1.5	-	Testing of dielectrics and composites	>32
[101]	~ 1.5	-	Characterisation of dielectric samples	very low
[102]	~ 2.5	0.25×0.42	Liquid sensing	-

14. Future Challenges of SIW

Current research in SIW technology is mostly in the microwave bands (that is, 300 MHz to 30 GHz). Although a few researchers have reported SIW devices that operate in the millimetre-wave bands, up to 60 GHz [90], research beyond 60 GHz in this field is still a huge challenge. Hence, future research in substrate-integrated waveguide devices will have to focus on the deployment of millimetre-wave devices within the frequency range of 60 to 300 GHz. Even when such devices are successfully designed/implemented, fabricating them in the workshop will also pose another huge challenges due to their enormous compact size. The authors of this paper believe that the best way to overcome these future challenges, and deploy SIW millimetre-wave devices of up to 300 GHz operating frequency, would be by collaborative research involving researchers from various fields. The system-in-package research concept may just be where the breakthrough may come from, sooner rather than later.

15. Conclusions

A review of the twenty-first century substrate-integrated waveguide is presented in this paper. The evolution of the SIW and its applications in the design of RF, microwave and millimetre-wave filtering components are covered. The SIW transmission line implements the conventional waveguide structure in planar form. It compensates for the demerits of microstrip structures at microwave and millimetre-wave circuit designs, and reduces the complexities associated with device fabrication. It is also less expensive when compared to the traditional waveguide structures. The SIW is the current state-of-the-art in the microwave and millimetre-wave field of research. A tabular comparison of the benefits of SIW components over planar (e.g., microstrip) and waveguide components is given in Table 6.

Table 6. Comparison of SIW components with planar and waveguide components.

Planar Components	Waveguide Components	SIW Components
Very good for low frequency applications but ineffective for millimetre-wave systems	Ideal for high frequency applications and systems	Works for both low and high frequency applications
Require rigorous production concessions when implemented at high frequencies	Difficult to manufacture	Moderately easy to manufacture both at low and high frequencies
Cost effective Easy to integrate with other planar devices	Very expensive Difficult to integrate with planar devices	Moderately cost effective Easy to integrate with planar devices
Very compact but suffers from high radiation loss	Very bulky though with minimal radiation loss	Compact and enormously reduced radiation loss
Low-level of unloaded quality factor	High-level of unloaded quality factor	Very good level of unloaded quality factor
Low-level of power processing capability	High-level of power processing capability	Very good level of power processing capability

Author Contributions: A.O.N. and E.R.O. have contributed equally to manuscript. All authors have read and agreed to the published version of the manuscript.

Funding: This research received no external funding.

Conflicts of Interest: The authors declare no conflict of interest.

References

- Chen, X.-P.; Wu, K. Substrate integrated waveguide filter: Basic design rules and fundamental structure features. *IEEE Microw. Mag.* **2014**, *15*, 108–116. [[CrossRef](#)]
- Hong, J.-S. *Microstrip Filters for RF/Microwave Applications*, 2nd ed.; Wiley: New York, NY, USA, 2011; pp. 1–635.

3. Nwajana, A.O.; Yeo, K.S.K. *Practical Approach to Substrate Integrated Waveguide (SIW) Diplexer: Emerging Research and Opportunity*, 1st ed.; IGI Global: Hershey, PA, USA, 2020; pp. 1–171.
4. Deslandes, D.; Wu, K. Design consideration and performance analysis of substrate integrated waveguide components. In Proceedings of the 32nd European Microwave Conference (EuMC), Milan, Italy, 27–29 September 2002; IEEE: Piscataway, NJ, USA, 2002; pp. 23–26.
5. Cassivi, Y.; Perregrini, L.; Arcioni, P.; Bressan, M.; Wu, K.; Conciauro, G. Dispersion characteristics of substrate integrated rectangular waveguide. *IEEE Microw. Wirel. Compon. Lett.* **2002**, *12*, 333–335. [[CrossRef](#)]
6. Nwajana, A. Analysis and Design of a Substrate Integrated Waveguide Multi-Coupled Resonator Diplexer. Ph.D. Thesis, University of East London, London, UK, July 2017; pp. 1–175.
7. Deslandes, D.; Wu, K. Single-substrate integrated technique of planar circuits and waveguide filters. *IEEE Trans. Microw. Theory Tech.* **2003**, *51*, 593–596. [[CrossRef](#)]
8. Venanzoni, G.; Mencarelli, D.; Morini, A.; Farina, M.; Prudenzeno, F. Review of substrate integrated waveguide circuits for beam-forming networks working in X-band. *Appl. Sci.* **2019**, *9*, 1003. [[CrossRef](#)]
9. Wu, K. Integration and interconnect techniques of planar and nonplanar structures for microwave and millimeter-wave circuits: Current status and future trend. In Proceedings of the 2001 Asia-Pacific Microwave Conference (APMC), Taipei, Taiwan, 3–6 December 2001; IEEE: Piscataway, NJ, USA, 2002; pp. 411–416.
10. Nwajana, A.O.; Yeo, K.S.K.; Dainkeh, A. Low cost SIW Chebyshev bandpass filter with new input/output connection. In Proceedings of the 16th Mediterranean Microwave Symposium (MMS), Abu Dhabi, UAE, 14–16 November 2016; IEEE: Piscataway, NJ, USA, 2017; pp. 1–4.
11. Cheng, Y.J. *Substrate Integrated Antennas and Arrays*, 1st ed.; CRC Press: New York, NY, USA, 2015; pp. 1–256.
12. Han, S.H.; Wang, X.L.; Fan, Y.; Yang, Z.Q.; He, Z.N. The generalized Chebyshev substrate integrated waveguide diplexer. *Prog. Electromagn. Res.* **2007**, *73*, 29–38. [[CrossRef](#)]
13. Deslandes, D.; Wu, K. Accurate modelling, wave mechanisms, and design considerations of a substrate integrated waveguide. *IEEE Trans. Microw. Theory Tech.* **2006**, *54*, 2516–2526. [[CrossRef](#)]
14. Bozzi, M.; Georgiadis, A.; Wu, K. Review of substrate-integrated waveguide circuits and antennas. *IET Microw. Antennas Propag.* **2011**, *5*, 909–920. [[CrossRef](#)]
15. Xu, F.; Wu, K. Guided-wave and leakage characteristics of substrate integrated waveguide. *IEEE Trans. Microw. Theory Tech.* **2005**, *53*, 66–73.
16. Chen, X.; Hong, W.; Cui, T.; Wu, K. Substrate integrated waveguide (SIW) linear phase filter. *IEEE Microw. Wirel. Compon. Lett.* **2005**, *15*, 787–789. [[CrossRef](#)]
17. Nwajana, A.O.; Dainkeh, A.; Yeo, K.S.K. Substrate integrated waveguide (SIW) diplexer with novel input/output coupling and no separate junction. *Prog. Electromagn. Res. M* **2018**, *67*, 75–84. [[CrossRef](#)]
18. Deslandes, D. Design equations for tapered microstrip-to-substrate integrated waveguide transitions. In Proceedings of the IEEE MTT-S International Microwave Symposium (IMS) Digest, Anaheim, CA, USA, 23–28 May 2010; pp. 704–707.
19. Deslandes, D.; Wu, K. Integrated microstrip and rectangular waveguide in planar form. *IEEE Microw. Wirel. Compon. Lett.* **2001**, *11*, 68–70. [[CrossRef](#)]
20. Deslandes, D.; Wu, K. Integrated transition of coplanar to rectangular waveguides. In Proceedings of the IEEE MTT-S International Microwave Symposium (IMS) Digest, Phoenix, AZ, USA, 20–25 May 2001; pp. 619–622.
21. Deslandes, D.; Wu, K. Analysis and design of current probe transition from grounded coplanar to substrate integrated rectangular waveguides. *IEEE Trans. Microw. Theory Tech.* **2005**, *53*, 593–596. [[CrossRef](#)]
22. Huang, Y.; Wu, K.L. A broad-band LTCC integrated transition of laminated waveguide to air-filled waveguide for millimeter-wave applications. *IEEE Trans. Microw. Theory Tech.* **2003**, *51*, 1613–1617. [[CrossRef](#)]
23. Xia, L.; Xu, R.; Yan, B.; Li, J.; Guo, Y.; Wang, J. Broadband transition between air-filled waveguide and substrate integrated waveguide. *Electron. Lett.* **2006**, *42*, 1403–1405. [[CrossRef](#)]
24. Ding, Y.; Wu, K. Substrate integrated waveguide-to-microstrip transition in multilayer substrate. *IEEE Trans. Microw. Theory Tech.* **2007**, *55*, 2839–2844. [[CrossRef](#)]
25. Bozzi, M.; Pasian, M.; Perregrini, L.; Wu, K. On the losses in substrate-integrated waveguides and cavities. *Int. J. Microw. Wirel. Technol.* **2009**, *1*, 395–401. [[CrossRef](#)]
26. Bozzi, M.; Perregrini, L.; Wu, K. Modeling of conductor, dielectric, and radiation losses in substrate integrated waveguide by the boundary integral-resonant mode expansion method. *IEEE Trans. Microw. Theory Tech.* **2008**, *56*, 3153–3161. [[CrossRef](#)]
27. Bozzi, M.; Perregrini, L.; Wu, K. Modeling of losses in substrate integrated waveguide by the boundary integral-resonant mode expansion method. In Proceedings of the IEEE MTT-S International Microwave Symposium (IMS) Digest, Atlanta, GA, USA, 15–20 June 2008; pp. 515–518.
28. Ranjkesh, N.; Shahabadi, M. Loss mechanism in SIW and MSIW. *Prog. Electromagn. Res. B* **2008**, *4*, 299–309. [[CrossRef](#)]
29. Bozzi, M.; Pasian, M.; Perregrini, L.; Wu, K. On the losses in substrate integrated waveguides. In Proceedings of the European Microwave Conference (EuMC), Munich, Germany, 9–12 October 2007; IEEE: Piscataway, NJ, USA, 2007; pp. 384–387.
30. Bozzi, M.; Pasian, M.; Perregrini, L. Modeling of losses in substrate integrated waveguide components. In Proceedings of the IEEE International Conference on Numerical Electromagnetic Modeling and Optimization for RF, Microwave, and Terahertz Applications (NEMO), Pavia, Italy, 14–16 May 2014; pp. 1–4.

31. Bozzi, M.; Perregrini, L.; Wu, K.; Arcioni, P. Current and future research trends in substrate integrated waveguide technology. *Radioengineering* **2009**, *18*, 201–209.
32. Pasian, M.; Bozzi, M.; Perregrini, L. Radiation losses in substrate integrated waveguides: A semi-analytical approach for a quantitative determination. In Proceedings of the IEEE MTT-S International Microwave Symposium (IMS) Digest, Seattle, WA, USA, 2–7 June 2013; pp. 1–3.
33. Chen, X.-P.; Wu, K. Substrate integrated waveguide filter: Practical aspects and design considerations. *IEEE Microw. Mag.* **2014**, *15*, 75–83. [[CrossRef](#)]
34. Wang, C. Temperature compensations for microwave resonators and filters. In Proceedings of the IEEE MTT-S International Microwave Symposium (IMS) Digest, Long Beach, CA, USA, 13–19 June 2005; pp. 1–30.
35. Djerafi, T.; Wu, K.; Deslandes, D. Temperature drift compensation technique for substrate integrated waveguide oscillator. *IEEE Microw. Wirel. Compon. Lett.* **2012**, *60*, 489–491. [[CrossRef](#)]
36. Djerafi, T.; Wu, K.; Deslandes, D. A temperature-compensation technique for substrate integrated waveguide cavities and filters. *IEEE Trans. Microw. Theory Tech.* **2012**, *60*, 2448–2455. [[CrossRef](#)]
37. Mansour, R.R.; Jolley, B.; Ye, S.; Thomson, F.S.; Dokas, V. On the power handling capability of high temperature superconductive filters. *IEEE Trans. Microw. Theory Tech.* **1996**, *44*, 1322–1338. [[CrossRef](#)]
38. Yu, M. Power-handling capability for RF filters. *IEEE Microw. Mag.* **2007**, *8*, 88–97. [[CrossRef](#)]
39. Wu, K.; Bozzi, M.; Fonseca, N.J.G. Substrate integrated transmission lines: Review and applications. *IEEE J. Microw.* **2021**, *1*, 345–363. [[CrossRef](#)]
40. Bozzi, M.; Perregrini, L.; Tomassoni, C. A review of compact substrate integrated waveguide (SIW) interconnects and components. In Proceedings of the IEEE 23rd Workshop on Signal and Power Integrity (SPI), Chambéry, France, 18–21 June 2019; pp. 1–4.
41. Wang, Z.; Shen, D.; Xu, R.; Yan, B.; Lin, W.; Guo, Y.; Xie, X. Partial H-plane bandpass filters based on substrate integrated folded waveguide (SIFW). In Proceedings of the IEEE Asia Pacific Microwave Conference (APMC), Singapore, 7–10 December 2009; pp. 1–4.
42. Grigoropoulos, N.; Sanz-Izquierdo, B.; Young, P.R. Substrate integrated folded waveguides (SIFW) and filters. *IEEE Microw. Wirel. Compon. Lett.* **2005**, *15*, 829–831. [[CrossRef](#)]
43. Wang, Z.; Bu, S.; Luo, Z. A substrate integrated folded waveguide (SIFW) H-plane band-pass filter with double H-plane septa based on LTCC. *IEEE Trans. Ultrason. Ferroelectr. Freq. Control.* **2012**, *59*, 560–563. [[CrossRef](#)]
44. Zhai, G.H.; Hong, W.; Wu, K.; Chen, J.X.; Chen, P.; Tang, H.J. Substrate integrated folded waveguide (SIFW) narrow-wall directional coupler. In Proceedings of the IEEE International Conference on Microwave and Millimeter Wave Technology, Nanjing, China, 21–24 April 2008; pp. 1–4.
45. Moro, R.; Moscato, S.; Bozzi, M.; Perregrini, L. Substrate integrated folded waveguide filter with out-of-band rejection controlled by resonant-mode suppression. *IEEE Microw. Wirel. Compon. Lett.* **2015**, *25*, 214–216. [[CrossRef](#)]
46. Qiu, P.-J.; Wang, Z.-G.; Yan, B. Novel Ka-band substrate integrated folded waveguide (SIFW) Quasi-elliptic filters in LTCC. In Proceedings of the IEEE Asia Pacific Microwave Conference (APMC), Hong Kong, China, 16–20 December 2008; pp. 1–4.
47. Alotaibi, S.K.; Hong, J.-S. Substrate integrated folded-waveguide filter with asymmetrical frequency response. In Proceedings of the 38th European Microwave Conference (EuMC), Amsterdam, The Netherlands, 27–31 October 2008; IEEE: Piscataway, NJ, USA, 2008; pp. 1002–1005.
48. Chien, H.-Y.; Shen, T.-M.; Hung, T.-Y.; Wu, R.-B. Design of a vertically stacked substrate integrated folded-waveguide resonator filter in LTCC. In Proceedings of the IEEE Asia Pacific Microwave Conference (APMC), Bangkok, Thailand, 11–14 December 2007; pp. 1–4.
49. Zhu, F.; Luo, G.Q.; Liao, Z.; Dai, X.W.; Wu, K. Compact dual-mode bandpass filters based on half-mode substrate-integrated waveguide cavities. *IEEE Microw. Wirel. Compon. Lett.* **2021**, *31*, 441–444. [[CrossRef](#)]
50. Hong, W.; Liu, B.; Wang, Y.; Lai, Q.; Tang, H.; Yin, X.X.; Dong, Y.D.; Zhang, Y.; Wu, K. Half mode substrate integrated waveguide: A new guided wave structure for microwave and millimeter wave application. In Proceedings of the Joint 31st International Conference on Infrared Millimeter Waves and 14th International Conference on Terahertz Electronics, Shanghai, China, 18–22 September 2006; p. 219.
51. Elobied, A.A.; Yang, X.-X.; Lou, T.; Gao, S. Compact 2×2 MIMO antenna with low mutual coupling based on half mode substrate integrated waveguide. *IEEE Trans. Antennas Propag.* **2021**, *69*, 2975–2980. [[CrossRef](#)]
52. Peng, Y.; Sun, L. A compact broadband phase shifter based on HMSIW evanescent mode. *IEEE Microw. Wirel. Compon. Lett.* **2021**, *31*, 857–860. [[CrossRef](#)]
53. Ji, L.; Li, X.-C.; He, X.; Mao, J.-F. A slow wave ridged half-Mode substrate integrated waveguide with spoof surface plasmon polaritons. *IEEE Trans. Plasma Sci.* **2021**, *49*, 1818–1825. [[CrossRef](#)]
54. Javanbakht, N.; Amaya, R.E.; Shaker, J.; Syrett, B. Side-lobe level reduction of half-mode substrate integrated waveguide leaky-wave antenna. *IEEE Trans. Antennas Propag.* **2021**, *69*, 3572–3577. [[CrossRef](#)]
55. Javanbakht, N.; Amaya, R.E.; Shaker, J.; Syrett, B. A compact cavity-based leaky-wave antenna in a low temperature co-fired ceramic process with improved performance. *IEEE Access* **2021**, *9*, 25014–25024. [[CrossRef](#)]
56. Bozzi, M.; Winkler, S.A.; Wu, K. Broadband and compact ridge substrate-integrated waveguides. *IET Microw. Antennas Propag.* **2010**, *4*, 1965–1973. [[CrossRef](#)]
57. Su, Y.; Lin, X.Q.; Fan, Y. Dual-polarized leaky wave antenna with low cross-polarization based on the mode composite ridged waveguide. In Proceedings of the International Conference on Microwave and Millimeter Wave Technology (ICMMT), Shanghai, China, 20–23 September 2020; pp. 1–3.

58. Che, W.; Li, C.; Zhang, D.; Chow, Y.L. Investigations on propagation and the band broadening effect of ridged rectangular waveguide integrated in a multilayer dielectric substrate. *IET Microw. Antennas Propag.* **2010**, *4*, 674–684. [[CrossRef](#)]
59. Liu, Z.; Lin, X.Q.; Su, Y. A novel compact diplexer with high isolation based on the mode composite ridged waveguide. In Proceedings of the International Conference on Microwave and Millimeter Wave Technology (ICMMT), Shanghai, China, 20–23 September 2020; pp. 1–3.
60. Zhang, F.; Hua, G. Empirical formulas of SIRW and its application in half-mode SIRW hybrid ring coupler design. In Proceedings of the IEEE MTT-S International Wireless Symposium (IWS), Shanghai, China, 20–23 September 2020; pp. 1–3.
61. Massoni, E.; Bozzi, M.; Wu, K. Increasing efficiency of leaky-wave antenna by using substrate integrated slab waveguide. *IEEE Antennas Wirel. Propag. Lett.* **2019**, *18*, 1596–1600. [[CrossRef](#)]
62. Bozzi, M.; Deslandes, D.; Arcioni, P.; Perregrini, L.; Wu, K.; Conciauro, G. Efficient analysis and experimental verification of substrate integrated slab waveguides for wideband microwave applications. *Int. J. RF Microw. Comput.-Aided Eng.* **2005**, *15*, 296–306. [[CrossRef](#)]
63. Massoni, E.; Silvestri, L.; Alaimo, G.; Marconi, S.; Bozzi, M.; Perregrini, L.; Auricchio, F. 3-D printed substrate integrated slab waveguide for single-mode bandwidth enhancement. *IEEE Microw. Wirel. Compon. Lett.* **2017**, *27*, 536–538. [[CrossRef](#)]
64. Deslandes, D.; Bozzi, M.; Arcioni, P.; Wu, K. Substrate integrated slab waveguide (SISW) for wideband microwave applications. In Proceedings of the IEEE MTT-S International Microwave Symposium (IMS) Digest, Philadelphia, PA, USA, 8–13 June 2003; pp. 1103–1106.
65. Bozzi, M.; Deslandes, D.; Arcioni, P.; Perregrini, L.; Wu, K.; Conciauro, G. Analysis of substrate integrated slab waveguides (SISW) by the BI-RME method. In Proceedings of the IEEE MTT-S International Microwave Symposium (IMS) Digest, Philadelphia, PA, USA, 8–13 June 2003; pp. 1975–1978.
66. Zhai, G.H.; Hong, W.; Wu, K.; Chen, J.X.; Chen, P.; Wei, J.; Tang, H.J. Folded half mode substrate integrated waveguide 3 dB coupler. *IEEE Microw. Wirel. Compon. Lett.* **2008**, *18*, 512–514. [[CrossRef](#)]
67. Nwajana, A.O.; Dainkeh, A.; Yeo, K.S.K. Substrate integrated waveguide (SIW) bandpass filter with novel microstrip-CPW-SIW input coupling. *J. Microw. Optoelectron. Electromagn. Appl.* **2017**, *16*, 393–402. [[CrossRef](#)]
68. Chen, X.-P.; Wu, K. Substrate integrated waveguide filter: Design techniques and structure innovations. *IEEE Microw. Mag.* **2014**, *15*, 121–133. [[CrossRef](#)]
69. Chu, P.; Hong, W.; Tuo, M.; Zheng, K.-L.; Yang, W.-W.; Xu, F.; Wu, K. Dual-mode substrate integrated waveguide filter with flexible response. *IEEE Trans. Microw. Theory Tech.* **2017**, *65*, 824–830. [[CrossRef](#)]
70. Mira, F.; Mateu, J.; Cogollos, S.; Boriaz, V.E. Design of ultra-wideband substrate integrated waveguide filters in zigzag topology. *IEEE Microw. Wirel. Compon. Lett.* **2009**, *19*, 281–283. [[CrossRef](#)]
71. Xie, H.-W.; Zhou, K.; Zhou, C.-X.; Wu, W. Compact SIW diplexer and dual-band bandpass filter with wide-stopband performances. *IEEE Trans. Circuits Syst. II Express Briefs* **2020**, *67*, 2933–2937. [[CrossRef](#)]
72. Xie, H.-W.; Zhou, K.; Zhou, C.-X.; Wu, W. Stopband-improved SIW triplexer and triple-band filters using alternatively cascaded triple- and single-mode cavities. *IEEE Access* **2019**, *7*, 56745–56752. [[CrossRef](#)]
73. Li, Q.; Yang, T. Compact UWB half-mode SIW bandpass filter with fully reconfigurable single and dual notched bands. *IEEE Trans. Microw. Theory Tech.* **2021**, *69*, 65–74. [[CrossRef](#)]
74. Song, K.; Zhou, Y.; Chen, Y.; Iman, A.M.; Patience, S.R.; Fan, Y. High-isolation diplexer with high frequency selectivity using substrate integrated waveguide dual-mode resonator. *IEEE Access* **2019**, *7*, 116676–116683. [[CrossRef](#)]
75. Xie, H.; Zhou, K.; Zhou, C.; Wu, W. Compact substrate-integrated waveguide triplexer based on a common triple-mode cavity. In Proceedings of the IEEE MTT-S International Microwave Symposium (IMS) Digest, Philadelphia, PA, USA, 10–15 June 2018; pp. 1–4.
76. Sirci, S.; Martinez, J.D.; Vague, J.; Boria, V.E. Substrate integrated waveguide diplexer based on circular triplet combline filters. *IEEE Microw. Wirel. Compon. Lett.* **2015**, *25*, 430–432. [[CrossRef](#)]
77. Iqbal, A.; Tiang, J.J.; Lee, C.K.; Lee, B.M. Tunable substrate integrated waveguide diplexer with high isolation and wide stopband. *IEEE Microw. Wirel. Compon. Lett.* **2019**, *29*, 456–458. [[CrossRef](#)]
78. Shehab, S.H.; Karmakar, N.C.; Walker, J. Substrate-integrated-waveguide power dividers: An overview of the current technology. *IEEE Antennas Propag. Mag.* **2020**, *62*, 27–38. [[CrossRef](#)]
79. Pradhan, N.C.; Subramanian, K.S.; Barik, R.K.; Cheng, Q.S. Design of compact substrate integrated waveguide based triple- and quad-band power dividers. *IEEE Microw. Wirel. Compon. Lett.* **2021**, *31*, 365–368. [[CrossRef](#)]
80. Liu, B.-G.; Lyu, Y.-P.; Zhu, L.; Cheng, C.-H. Compact square substrate integrated waveguide filtering power divider with wideband isolation. *IEEE Microw. Wirel. Compon. Lett.* **2021**, *31*, 109–112. [[CrossRef](#)]
81. Lai, J.; Yang, T.; Chi, P.-L.; Xu, R. A novel 1.7–2.85-GHz filtering crossover with independently tuned channel passbands and reconfigurable filtering power-dividing function. *IEEE Trans. Microw. Theory Tech.* **2021**, *69*, 2458–2469. [[CrossRef](#)]
82. Zhang, G.; Liu, Y.; Wang, E.; Yang, J. Multilayer packaging SIW three-way filtering power divider with adjustable power division. *IEEE Trans. Circuits Syst. II Express Briefs* **2020**, *67*, 3003–3007. [[CrossRef](#)]
83. Nwajana, A.O.; Ogbodo, E.A.; Imasuen, I.I. Formulation for energy distribution in T-junctions for diplexer design. In Proceedings of the IEEE 3rd International Conference on Electrical, Communication, and Computer Engineering (ICECCE), Kuala Lumpur, Malaysia, 12–13 June 2021; pp. 1–4.
84. Wang, C.; Wang, X.; Liu, H.; Chen, Z.; Han, Z. Substrate integrated waveguide filtenna with two controllable radiation nulls. *IEEE Access* **2020**, *8*, 120019–120024. [[CrossRef](#)]

85. Xie, H.-Y.; Wu, B.; Wang, Y.-L.; Fan, C.; Chen, J.-Z.; Su, T. Wideband SIW filtering antenna with controllable radiation nulls using dual-mode cavities. *IEEE Antennas Wirel. Propag. Lett.* **2021**, *20*, 1799–1803. [[CrossRef](#)]
86. Yin, J.-Y.; Bai, T.-L.; Deng, J.-Y.; Ren, J.; Sun, D.; Zhang, Y.; Guo, L.-X. Wideband single-layer substrate integrated waveguide filtering antenna with U-shaped slots. *IEEE Antennas Wirel. Propag. Lett.* **2021**, *20*, 1726–1730. [[CrossRef](#)]
87. Zhao, D.; Lin, F.; Sun, H.; Zhang, X.Y. A miniaturized dual-band SIW filtering antenna with improved out-of-band suppression. *IEEE Trans. Antennas Propag.* **2022**, *70*, 126–134. [[CrossRef](#)]
88. Li, L.; Wu, S.; Pang, D.; Zhang, X.; Wang, Q. A fifth-order single-layer dual-band half-mode SIW filtering antenna with a multifunctional single slot. *IEEE Antennas Wirel. Propag. Lett.* **2021**, *20*, 1676–1680. [[CrossRef](#)]
89. Kumar, A.; Althuwayb, A.A. SIW resonator-based duplex filtenna. *IEEE Antennas Wirel. Propag. Lett.* **2021**, *20*, 2544–2548. [[CrossRef](#)]
90. Hu, H.-T.; Chan, K.F.; Chan, C.H. 60 GHz Fabry–Perot Cavity filtering antenna driven by an SIW-fed filtering source. *IEEE Trans. Antennas Propag.* **2022**, *70*, 823–834. [[CrossRef](#)]
91. Lu, R.; Yu, C.; Wu, F.; Yu, Z.; Zhu, L.; Zhou, J.; Yan, P.; Hong, W. SIW cavity-fed filtennas for 5G millimeter-wave applications. *IEEE Trans. Antennas Propag.* **2021**, *69*, 5269–5277. [[CrossRef](#)]
92. Hu, H.-T.; Chan, C.H. Substrate-integrated-waveguide-fed wideband filtering antenna for millimeter-wave applications. *IEEE Trans. Antennas Propag.* **2021**, *69*, 8125–8135. [[CrossRef](#)]
93. Hu, M.; Yu, Z.; Xu, J.; Lan, J.; Zhou, J.; Hong, W. Diverse SRRs loaded millimeter-wave SIW antipodal linearly tapered slot filtenna with improved stopband. *IEEE Trans. Antennas Propag.* **2021**, *69*, 8902–8907. [[CrossRef](#)]
94. Dong, Y.; Itoh, T. Miniaturized substrate integrated waveguide slot antennas based on negative order resonance. *IEEE Trans. Antennas Propag.* **2010**, *58*, 3856–3864. [[CrossRef](#)]
95. Matbouly, H.E.; Boubekour, N.; Domingue, F. Passive microwave substrate integrated cavity resonator for humidity sensing. *IEEE Trans. Microw. Theory Tech.* **2015**, *63*, 4150–4156. [[CrossRef](#)]
96. Varshney, P.K.; Akhtar, M.J. Substrate integrated waveguide derived novel two-way rotation sensor. *IEEE Sens. J.* **2021**, *21*, 1519–1526. [[CrossRef](#)]
97. Yun, T.; Lim, S. High-Q and miniaturized complementary split ring resonator-loaded substrate integrated waveguide microwave sensor for crack detection in metallic materials. *Sens. Actuators A Phys.* **2014**, *214*, 25–30. [[CrossRef](#)]
98. Varshney, P.K.; Akhtar, M.J. Permittivity estimation of dielectric substrate materials via enhanced SIW sensors. *IEEE Sens. J.* **2021**, *21*, 12104–12112. [[CrossRef](#)]
99. Morales, H.L.; Chavez, A.C.; Murthy, D.V.B.; Olvera-Cervantes, J.L. Complex permittivity measurements using cavity perturbation technique with substrate integrated waveguide cavities. *Rev. Sci. Instrum.* **2010**, *81*, 1–4.
100. Varshney, P.K.; Tiwari, N.K.; Akhtar, M.J. SIW cavity based compact RF sensor for testing of dielectrics and composites. In Proceedings of the IEEE MTT-S International Microwave Symposium (IMS) Digest, New Delhi, India, 5–9 December 2016; pp. 1–4.
101. Varshney, P.K.; Akhtar, M.J. A compact planar cylindrical resonant RF sensor for the characterization of dielectric samples. *J. Electromagn. Waves Appl.* **2019**, *33*, 1700–1717. [[CrossRef](#)]
102. Morales, H.L.; Choi, J.H.; Lee, H.; Medina-Monroy, J.L. Compact dielectric-permittivity sensors of liquid samples based on substrate-integrated-waveguide with negative-order-resonance. *IEEE Sens. J.* **2019**, *19*, 8694–8699. [[CrossRef](#)]